

A NOVEL TECHNIQUE ON THE ANALYTICAL CALCULATION OF OPEN-CIRCUIT FLUX DENSITY DISTRIBUTION IN BRUSHLESS PERMANENT-MAGNET MOTOR

M. Moallem, A. Kiyomarsi and M. R. Hassanzadeh

*Department of Electrical and Computer Engineering, Isfahan University of Technology
P. O. Box 84154, Isfahan, Iran
moallem@cc.iut.ac.ir - kiyomarsi@electdp.iut.ac.ir - mrh_zadeh@qazviniau.ac.ir*

(Received: January 20, 2003 – Accepted in Revised Form: February 26, 2004)

Abstract Both the cogging and electromagnetic torques depends on the shape of the flux density distribution in the airgap region. A two-dimensional (2-D) analytical method for predicting the open-circuit airgap field distribution in brushless permanent magnet motors, considering the direction of magnetization, i.e., radial or parallel, and the effect of real shape of stator slot-openings is presented in this paper. It involves the solution of the governing field equations in polar coordinates in airgap and magnet regions. This method uses a new 2-D relative permeance function. For the comparison purposes, a 2-D finite element (FE) analysis is used for the analysis of a fully-pitched, double-layer windings brushless permanent-magnet (PM) drive. The results obtained by this method are very close to those obtained by FE analysis especially at the corner tips of the tooth.

Key Words Brushless Permanent Magnet Motor, Analytical Method, Finite Element Method

چکیده ضربانهای گشتاور وابسته به توزیع میدان الکترومغناطیسی در ماشینهای الکتریکی می‌باشند. بمنظور برآورد دقیق چگالی شار مغناطیسی در فاصله هوایی ماشین مغناطیس دائم بدون جاروبک، یک روش تحلیلی دو بعدی ارائه شده است. در این روش سعی بر کامل نمودن روشهای قبلی بوده و علاوه بر در نظر گرفتن اثر شکل شیارهای استاتور، جهت میدان القایی در مغناطیس دائم بصورت شعاعی و موازی مورد توجه قرار گرفته است. برای در نظر گرفتن اثر شیارها، یک تابع پرمیانس نسبی جدید مورد استفاده قرار گرفته است. این تابع، شامل دو متغیر است. از حیث دقت و توانایی، نتایج حاصل از این روش با نتایج عددی حاصل از روش المانهای محدود دو بعدی مورد مقایسه قرار گرفته است. برای انجام این مقایسه، یک ماشین مغناطیس دائم از نوع بدون جاروبک، چهار قطب و سه فاز شامل سی و شش دندانه در داخل استاتور، شبیه سازی شده است. نتایج بدست آمده بسیار نزدیک به نتایج حاصل از روش اجزاء محدود می‌باشد.

1. INTRODUCTION

Brushless permanent-magnet motors can be divided into the PM synchronous AC motor (PMSM) and PM brushless DC motor (PMBDCM). The former has sinusoidal airgap flux and back EMF, thus has to be supplied with sinusoidal current to produce constant torque. The PMBDCM has the trapezoidal back EMF, so the rectangular current waveform in its armature winding is required to obtain the low ripple torque [1,2]. Generally, the magnets with parallel magnetization are used in the PMSM while the magnets with radial magnetization are suitable for

the BDCM. The permanent magnet mounting in different motors with different magnet setting and direction of magnetization are compared in [3].

Torque ripple minimization in PM motors is conventionally obtained by either good motor design or appropriate control strategies. In design optimization programs, a reliable and detailed analysis of the torque and back EMF of the machine should be performed. In this paper a new permeance function is added to the Zhu's method to model the slot shape more realistically. Addition of the new permeance function caused the shape of flux distribution on the corner of the slots gets closer to those obtained by FE Method.

Boules developed a two-dimensional field analysis technique by which the magnet and armature fields of a surface-mounted brushless synchronous machine can be predicted [4]. The x- and y- components of the flux density at any point in the airgap or permanent magnet are calculated. The method has also been extended in polar coordinate that was used to predict the no-load flux density distribution on the stator and rotor surfaces of surface-mounted PM machines and also the amount of magnetic flux entering these surfaces [5]. Boules continued his work and presented an analytical solution of the airgap flux density distribution for the interior PM circumferentially-magnetized brushless permanent magnet motor [6].

In a comprehensive proposed model, Zhu *et al.* presented an analytical solution for predicting the resultant instantaneous magnetic field in the radially-magnetized BDCM and PMDC under any load condition and commutation strategy [7]. The armature reaction of BDCM motors is taken into account [8]. The effects of stator slots on the magnetic field distribution in air-gap/magnet region are considered via a 2-D relative permeance function [9]. Operation under any load conditions has also been completely investigated in [10]. They also presented a general analytical solution of the magnetic field in both surface-mounted and inset magnet brushless motors and also rotors with air spaces between interpole iron and magnets [11].

Rasmussen *et al.* [12] presented a new and general analytical method for the airgap magnetic fields in brushless and brushed PM motors with surface-mounted magnets, in which both the radial and tangential components of the magnetization are present.

Recently, Zhu *et al.* [13] extended Rasmussen's model to predict magnetic field due to the armature reaction both in the three phase overlapping and non-overlapping stator windings. This field distribution is a function of phase winding current waveform harmonics, the slot-opening factor, the winding distribution factor, winding pitch factor and the effect of curvature. The magnetic field produced by the surface-mounted magnets, both in the internal rotor and external rotor topologies and type of magnetization and also stator slotting effects have

been studied.

2. EFFECT OF STATOR SLOT OPENINGS

An effective method for modeling the influence of stator slots in the magnetic field distribution of PMBDCM with surface-mounted magnets is presented in [9]. The proposed 2-D function assumes infinitely deep rectilinear stator slots. This relative permeance function has a Fourier series of the form as:

$$\tilde{\lambda}_K(\alpha, r) = \sum_{n=0}^{\infty} \tilde{\Lambda}_n(r, K) \text{Cos}[nQ_s(\alpha + \alpha_{sa})] \quad (1)$$

This initial relative permeance function (Figure 1-a) has been used to investigate a little more realistic stator teeth, as shown in Figure 1-b. Each stator slot can be extracted from the initial model via addition of two new virtual stator slots, i.e., A1 and A2 areas as shown in Figure 1-b.

Therefore, the relative permeance of the real stator slots can be calculated as follows:

$$\tilde{\lambda}(\alpha, r) = \tilde{\lambda}_0(\alpha, r) - \tilde{\lambda}_1(\alpha, r) - \tilde{\lambda}_2(\alpha, r) \quad (2)$$

The reference for the α (in $\tilde{\lambda}_0(\alpha, r)$), i.e. $\alpha = 0$, is the axis of the phase A winding. To take into account stator slots and magnetic saturation, the airgap g , can be increased to $g'' = g(K_c K_s)$, where K_c and K_s are Carter's coefficient and saturation factor respectively. Leakage inductance and phase resistance are considered as described in [14,15].

3. FIELD DISTRIBUTION MODELLING

A 2-D analytical model for calculating the field distribution in the airgap region of surface-mounted permanent magnet brushless motors has been developed. In this method each magnet is divided to equivalent surface current sheets and it is notable that because of uniform magnetization of magnets, the volume current density distribution is

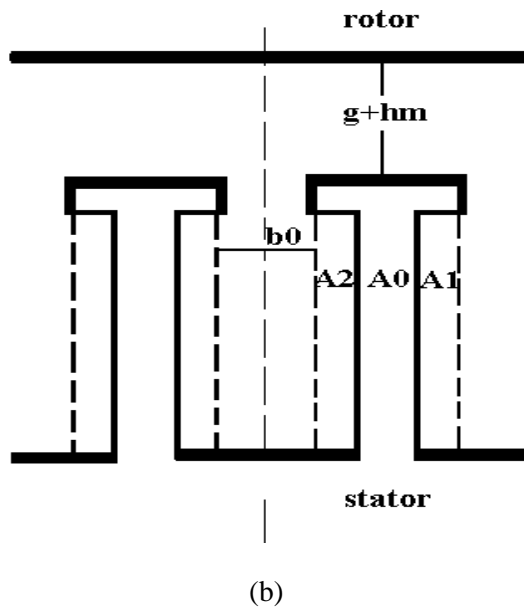
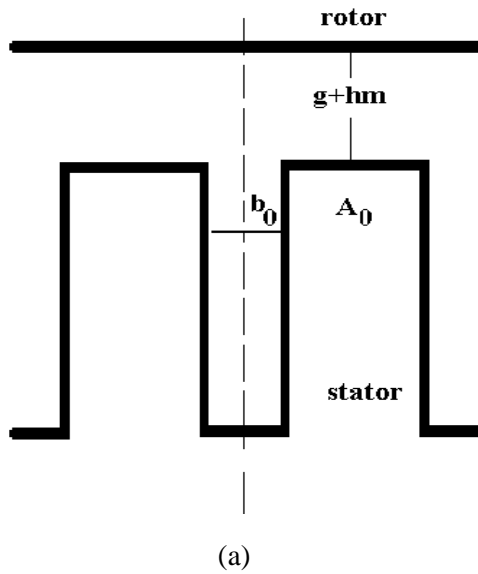


Figure 1. Permeance model (a) initial model and (b) new model.

equal to zero. These current sheets are divided to some thin coils, and the resultant field at any point can be calculated by integrating the fields produced by each of these thin individual coils into which infinitesimal current carried.

Both the radially magnetized and parallel magnetization are considered. Equation 3 has described the calculation of open-circuit field

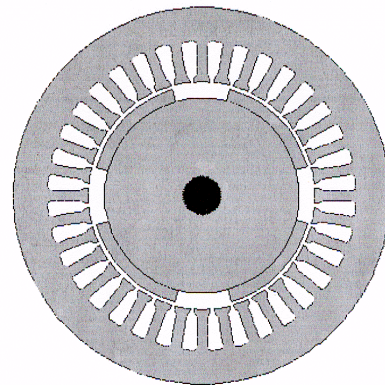


Figure 2. Cross-section of machine.

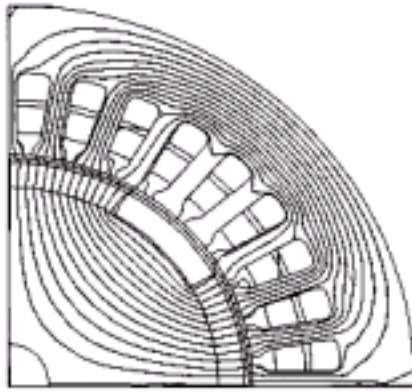
distribution:

$$B_{open-circuit}(r, \alpha, t) = B_{magnet}(r, \alpha, t) \tilde{\lambda}(r, \alpha) \quad (3)$$

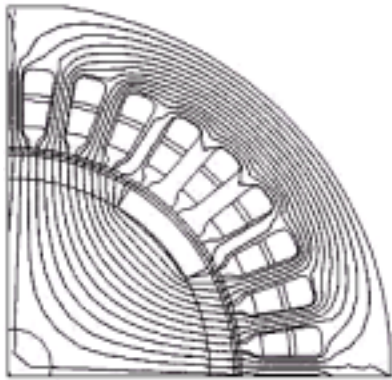
4. SIMULATION RESULTS

Cross section of the 5 HP, 1500 rpm, 4-pole SPMSM motor [16], is shown in Figure 2. The PM motor is a 3-phase, 36 slot brushless motor. Rotor and stator are of ferromagnetic materials, M-19 and M-36, and the PM excitation consists of Nd-Fe-B (N33) PMs. Figure 3 shows comparison of flux lines in both radial and parallel magnetizations. Figures 4 and 5 show comparison of analytical and numerical results.

Magnetic saturation is considered in FE method more precisely; however, neglecting the magnetic saturation, has no considerable effect due to large airgap length. As a result, the analytical model is a powerful tool for torque pulsation calculations, using magnetic flux density distributions in the mid-airgap. Also average torque can be obtained using effective flux per pole and unit length of stator. As shown in Table 1, the finite element analysis results and the results by previous method and the new improved method for the value of flux per pole per length of the stator have been presented for comparison. The improvement obtained, is clear as compares with FE results especially at the corners of the teeth.



(a)



(b)

Figure 3. Equipotential lines: Instantaneous flux distribution due to magnets acting alone (open-circuit condition) at time $t = 0$. (a) Radial Magnetization and (b) Parallel Magnetization.

5. COMPARISON OF DIFFERENT METHODS

To evaluate the new method, a comparison between lumped – parameter and distributed-parameter flux calculations is carried out [17-20]. In this way, the Equations 4-6 may be usefully modeled and different approaches are compared. A more accurate model of the flux distributions in the airgap region is obtained by solving the magnetic equivalent circuit (MEC) model of machine which takes into account the non-linear DC BH-characteristics of the iron parts of the machine as shown in Figure 6.

The fundamental component of flux density

distribution obtained from MEC analysis (B1:MEC), the new two-dimensional polar-based coordinates method (B2:2DP), the two-dimensional Cartesian-based coordinates method (B3:2DR), the two-dimensional polar-based coordinates method with stator slot effects (B4:2DS), and also that obtained from FEM analysis (B5:FEM), are compared in Table 2 underlines these by showing the peak of fundamental component of flux density distribution. The expressions for calculation of these can be written as:

$$\hat{B}_1^1 = \frac{4}{\pi} B_s \sin\left(\frac{\alpha_e \pi}{2}\right) \quad (4)$$

$$\hat{B}_1^2 = \frac{4}{\pi} B_r \frac{\sin\left(\frac{\alpha_e \pi}{2}\right)}{CN} \quad (5)$$

$$CN = \cosh\left(\frac{\pi g''}{\tau}\right) +$$

$$\frac{\mu_M}{\mu_0} \sinh\left(\frac{\pi g''}{\tau}\right) \coth\left(\frac{\pi h M}{\tau}\right)$$

in the above expressions, the effective geometrical length of airgap ($g' = K_c g$) and the effective magnetic length of airgap ($g'' = K_s g'$) are considered and saturation factor, K_s , is given by:

$$K_s = 1.0 + \frac{M_{Fe}}{M_{airgap}} \quad (6)$$

where M_{Fe} and M_{Airgap} are the total MMF required to overcome the iron and airgap reluctances respectively. Because of the nonlinearity of the magnetization characteristic of the iron parts of the motor, an iterative algorithm for the saturation factor determination is required. A solution is reached if the permeabilities of all iron segments show only slight change in two successive iterations. \hat{B}_1^4 and \hat{B}_1^5 are the peak of fundamental component of $B_{open_circuit}(r, \alpha, t)$ and FEM results, respectively.

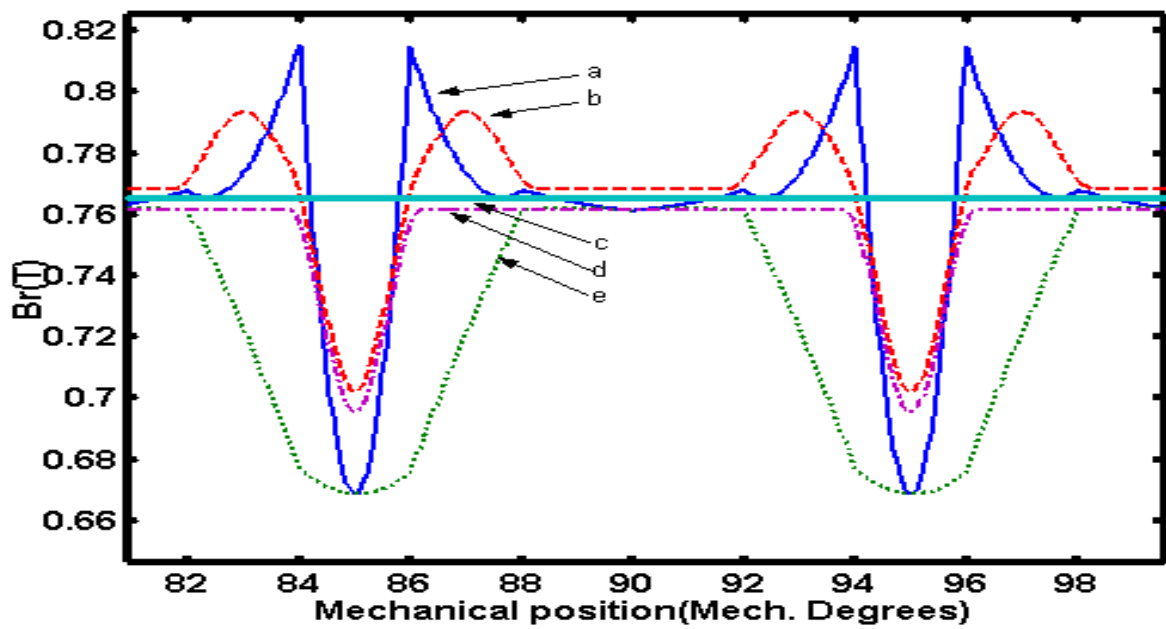
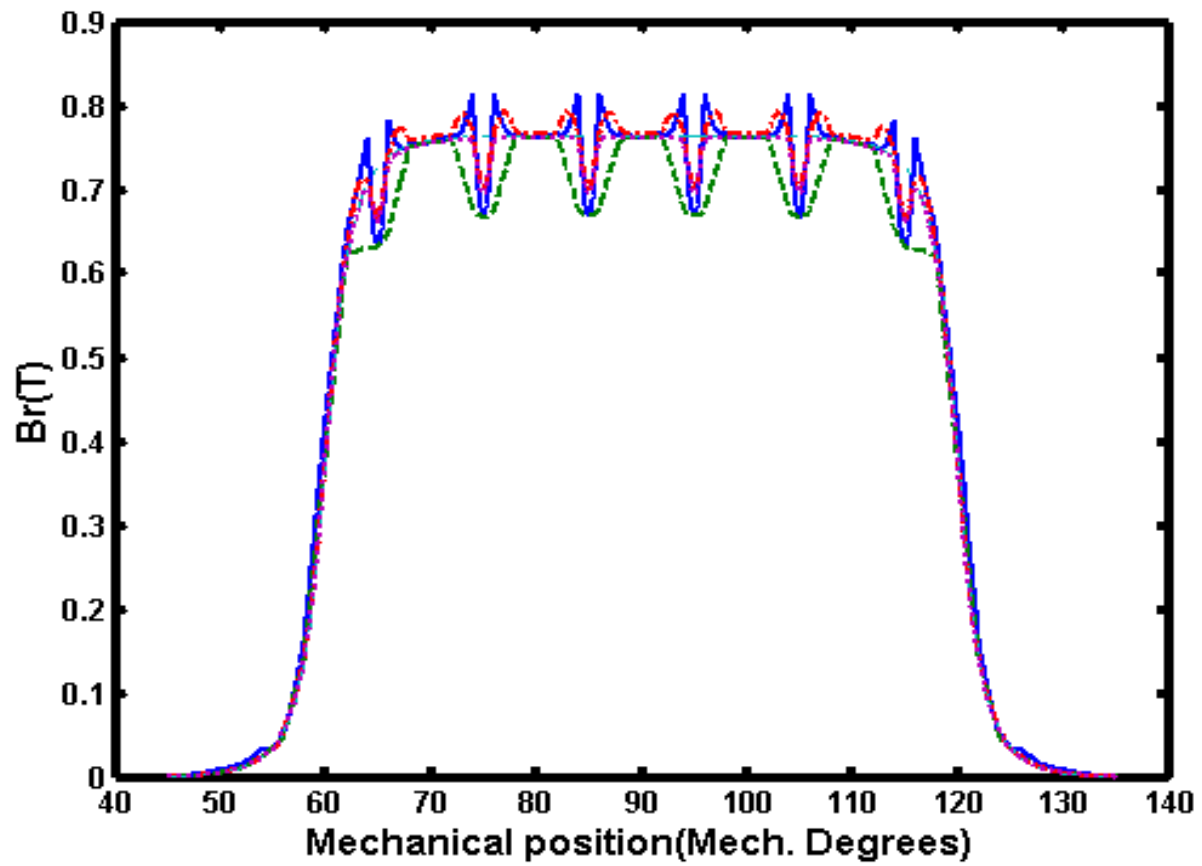


Figure 4. Flux density distribution Radial Magnetization: (a) Bsum(FEM), (b) Bocn, (c)- Bocnb, (d) Boco and (e) Br(FEM).

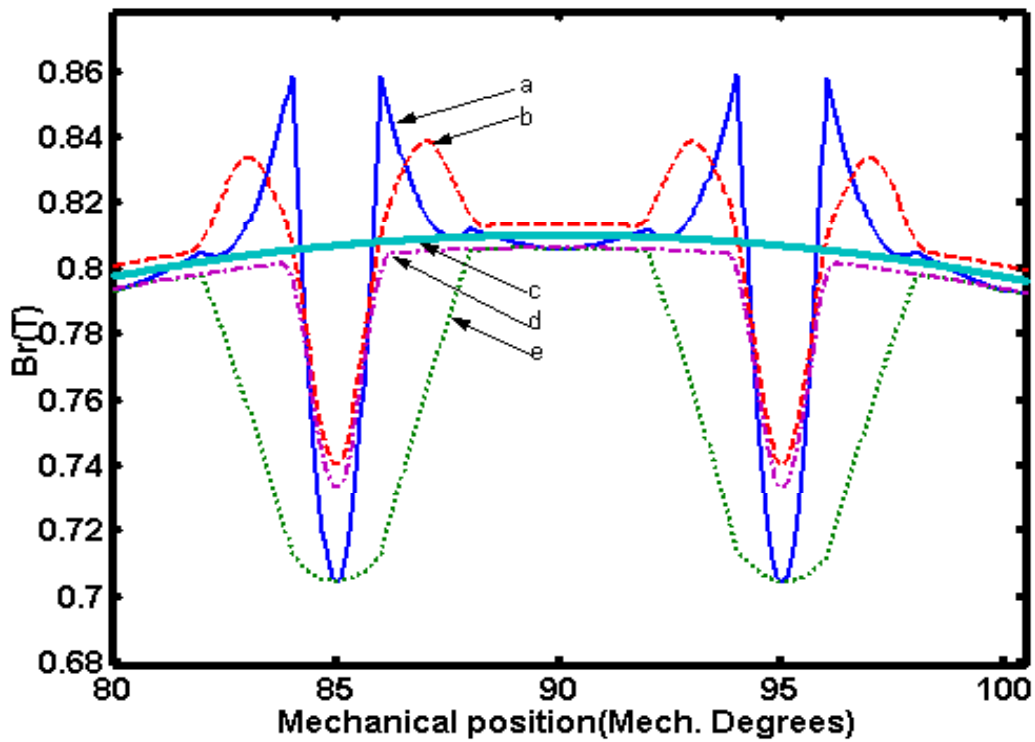
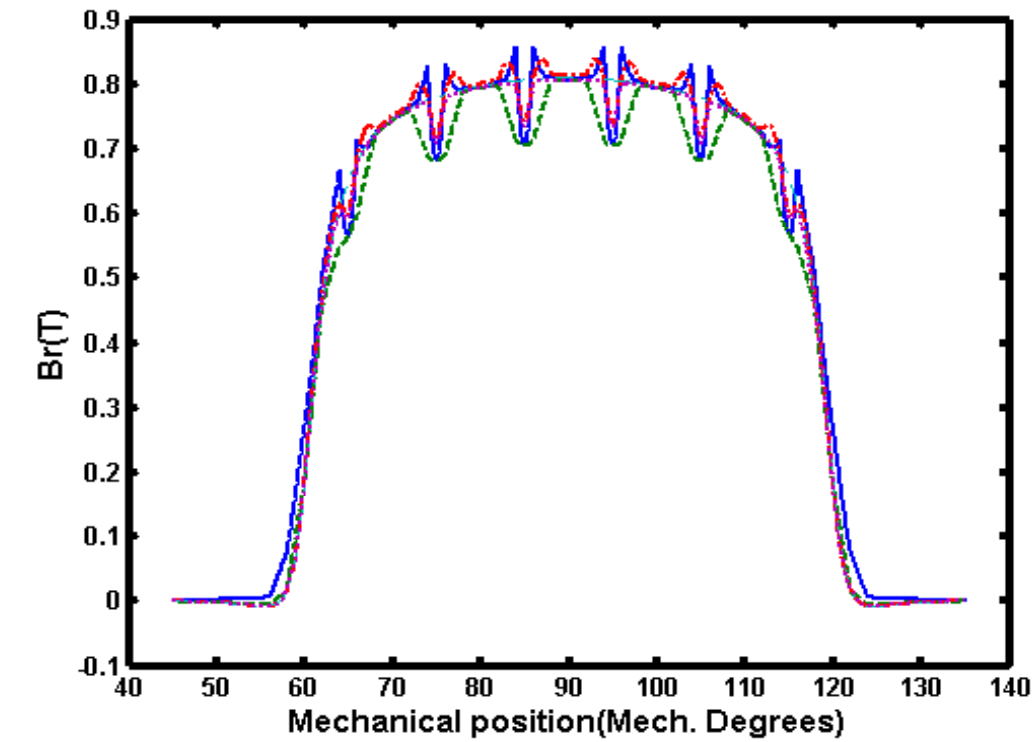


Figure 5. Flux density distribution Parallel Magnetization: (a) $B_{sum}(FEM)$, (b) B_{ocn} , (c) B_{ocnb} , (d) B_{oco} and (e) $B_r(FEM)$.

TABLE 1. Flux Entering the Stator Pole.

	Parallel Magnetization (mWb/m)	Radial Magnetization (mWb/m)
Boules' Method	44.76	46.86
New Method	44.09	46.16
FEM	42.32	44.43

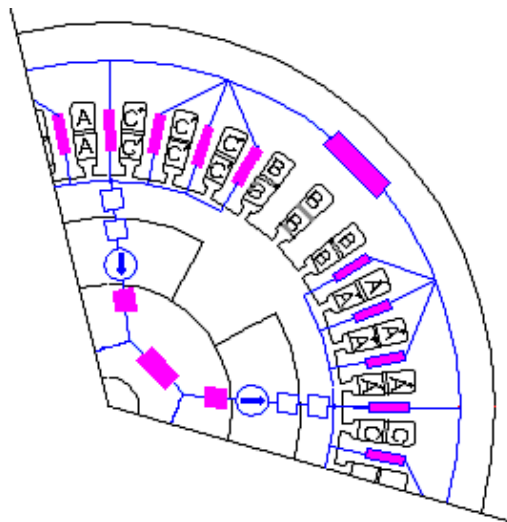


Figure 6. Magnetic Equivalent Circuit model Non-Linear elements are in black.

6. CONCLUSION

By addition of new permeance to the 2-D analytical model of PMBLDC motor, an improvement in the field distribution of the motor is obtained. The improved permeance model for the calculation of no-load flux density distribution in the airgap and the finite element analysis results, are compared. The good agreement of the flux curves obtained by the analytical method and FE results has proved the validity of this method which can be used for fast calculation of back-EMF and torque ripples which are required in the design and shape optimization process of the machine.

TABLE 2. Comparison of Different Field Calculation Methods.

	Parallel Magnetization (T)	Radial Magnetization (T)
B1(MEC)	-----	0.8200
B2(2DR)	-----	0.8795
B3(2DP)	0.8262	0.8385
B4(2DS)	0.8138	0.8260
B5(FEM)	0.7818	0.7953

Flux densities are in Tesla.

7. LIST OF SYMBOLS

α	Angular displacement between the stator MMF and rotor MMF
α_{sa}	Angular displacement between the stator slot axis and the axis of the coils of phase A
$\tilde{\lambda}$	Relative permeance function
Λ_{ref}	Reference permeance
B_0	Stator slot-opening
B_{magnet}	Flux density due to magnet at stator inside surface
$B_{open-circuit}$	Open-circuit flux density distribution
B_{ocn}	Open-circuit flux density; New method
B_{ocb}	Open-circuit flux density; Boules' method
B_{oco}	Open-circuit flux density; Only assuming $\tilde{\lambda}_0$
B_r	Radial component of flux density; obtained by FEM analysis
B_{sum}	Absolute resultant open-circuit flux density
P	Pole number
Q_s	Stator slot number

8. APPENDIX I

Prototype Brushless Pm Motor Parameters

Stator

Outer radius (r_{so}) 97.1 mm

Inner radius (r_{si})	58.5 mm
Length (l_s)	76.0 mm
Yoke depth (h_y)	17.4 mm
Tooth depth (h_t)	17.2 mm
Tooth top thickness (h_{tt})	2.0 mm
Number of slots	36
Slot opening (b_o)	5.1 mm
Lamination material	Steel M36
fully processed-29 Gage	
Winding	Double-layer, Fully-Pitched
Stator turns per phase (N_s)	96 turns

Rotor

Outer radius (r_{ro})	56.5 mm
Inner radius (r_{ri})	50.2 mm
Length (l_r)	76.0 mm
Number of poles (2p)	4
Lamination material	Steel M19
fully processed-29 Gage	
Magnet material	N33
Remanence (B_{res})	1.1 T
Relative recoil permeability (μ_r)	1.05
Magnet height (h_m)	6.3 mm
Magnet arc angle ($2\alpha_m$)	60 Mech. degrees

9. REFERENCES

- Hendershot Jr., J. R. and Miller, T. J. E., "Design of Brushless Permanent-Magnet Motors", Magna Physics Publishing and Clarendon Press, Oxford, (1994).
- Johns, T. M. and Soong, W. L., "Pulsating Torque Minimization Techniques for Permanent Magnet AC Motor Drives- A Review", *IEEE Transactions on Industrial Electronics*, Vol. 43, No. 2, (1996), 321-330.
- Cai, W., Fulton, D. and Reichert, K., "Design of Permanent Magnet Motors with Low Torque Ripples: A Review", *ICEM 2000*, ESPO, Finland, (2000), 1384-1388.
- Boules, N., "Two-Dimensional Field Analysis of Cylindrical Machines with Permanent Magnet Excitation", *IEEE Transactions on Industry Applications*, Vol. IA-20, (September/October 1984), 1267-1277.
- Boules, N., "Prediction of No-Load Flux Density Distribution in Permanent Magnet Machines", *IEEE Transactions on Industry Applications*, Vol. IA-21, (1985), 633-643.
- Boules, N., "Field Analysis of PM Synchronous Machines with Buried Magnet Rotor", General Motors Research Laboratories, Warren, MI 48090-9055, (1986), 1063-1066.
- Zhu, Z. Q., Howe, D., Bolte, E. and Ackermann, B., "Instantaneous Magnetic Field Distribution in Brushless Permanent Magnet DC Motors, Part I: Open-Circuit Field", *IEEE Transactions on Magnetics*, Vol. 29, No. 1, (January 1993), 124-135.
- Zhu, Z. Q. and Howe, D., "Instantaneous Magnetic Field Distribution in Brushless Permanent Magnet DC Motors, Part II: Armature-Reaction Field", *IEEE Transactions on Magnetics*, Vol. 29, No. 1, (January 1993), 136-142.
- Zhu, Z. Q. and Howe, D., "Instantaneous Magnetic Field Distribution in Brushless Permanent Magnet DC Motors, Part III: Effect of Stator Slotting", *IEEE Transactions on Magnetics*, Vol. 29, No. 1, (January 1993), 143-151.
- Zhu, Z. Q. and Howe, D., "Instantaneous Magnetic Field Distribution in Brushless Permanent Magnet DC Motors, Part VI: Magnetic Field on Load", *IEEE Transactions on Magnetics*, Vol. 29, No. 1, (January 1993), 152-158.
- Zhu, Z. Q., Howe, D. and Xia, Z. P., "Prediction of Open-Circuit Airgap Field Distribution in Brushless Machines Having an Inset Permanent Magnet Rotor Topology", *IEEE Transactions on Magnetics*, Vol. 30, No. 1, (January 1993), 98-107.
- Rasmussen, K. F., et al., "Analysis and Numerical Amputation of Air-Gap Magnetic Fields in Brushless Motors with Surface Permanent Magnets", *IEEE Transactions on Industry Applications*, Vol. 36, No.6, (November/December 2000), 1547-1550.
- Zhu, Z. Q., Howe, D. and Chan, C. C., "Improved Analytical Model for Predicting the Magnetic Field Distribution in Brushless Permanent-Magnet Machines", *IEEE Transactions on Magnetics*, Vol. 38, No. 8, (July 2002), 1500-1506.
- Boldea, I. and Nasar, S., "The Induction Machine Handbook", CRC Press, (2002).
- Gieras, J. F. and Piech, Z. J., "Linear Synchronous Motors, Transportation and Automation Systems", CRC Press, LLC, (2000).
- Slemon, G. R. and Liu, X., "Core Losses in Permanent Magnet Motors", *IEEE Transactions on Magnetics*, Vol. 26, No. 5, (September 1990), 1653-1655.
- Gol, O., et al., "Performance Prediction of a Permanent Magnet Generator using a Magnetic Circuit Model", *ICEM 2000*, (August 28-30, 2000), Espo Finland, (2000), 1280-1284.
- Rasmussen, C. B., "Modeling and Simulation of Surface Mounted PM Motors, Ph.D. Thesis, Aalborg University, Denmark, ISBN 87-89179-15-3, (1996).
- Cheng, M., et al., "Nonlinear Varying-Network Magnetic Circuit Analysis for Doubly Salient Permanent-Magnet Motors", *IEEE Transactions on Magnetics*, Vol. 36, No. 1, (January 2000), 339-348.
- US Steel Manual, "Non-Oriented Electrical Steel Sheets", Pittsburgh, Pa. 15230.

